AD-A183 969 ESTIMATES OF SATELLITE EHF COMMUNICATION OUTAGES DUE TO ATTENUATION BY RAIN(U) AIR FORCE GEOPHYSICS LAB HANSCOM AFB MA P TATTELMAN ET AL. 05 MAR 87 AFGL-TR-87-0001 1/1

UNCLASSIFIED F/G 20/14 NL

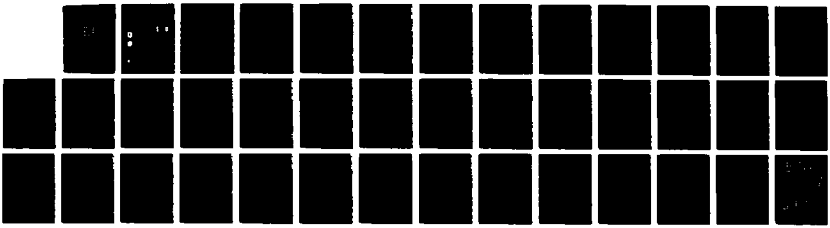

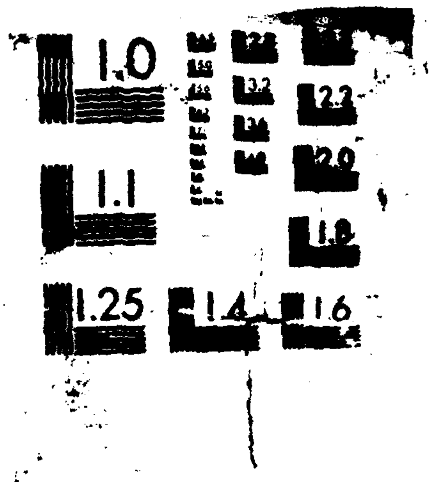

MICROCOPY RESOLUTION TEST CHART

(12)

AFGL-TR- 87-0081
ENVIRONMENTAL RESEARCH PAPERS, NO. 970

DTIC FILE COPY

AD-A183 969

Estimates of Satellite EHF Communication Outages Due to Attenuation by Rain

PAUL TATTELMAN
RICHARD W. KNIGHT
KATHRYN G. SCHARR

5 March 1987

Approved for public release; distribution unlimited.

ATMOSPHERIC SCIENCES DIVISION PROJECT 6670

AIR FORCE GEOPHYSICS LABORATORY
HANSCOM AFB, MA 01731

87 9 2 003

This report has been reviewed by the ESD Public Affairs Office (PA) and is releasable to the National Technical Information Service (NTIS).

"This technical report has been reviewed and is approved for publication"

FOR THE COMMANDER

DONALD D. GRANTHAM
Chief, Atmospheric Structure Branch

ROBERT A. McCLATCHEY
Director, Atmospheric Sciences Division

Unclassified
SECURITY CLASSIFICATION OF THIS PAGE

AD-A183969

REPORT DOCUMENTATION PAGE

Form Approved OMB No. 0704-0188

1a. REPORT SECURITY CLASSIFICATION Unclassified	1b. RESTRICTIVE MARKINGS
2a. SECURITY CLASSIFICATION AUTHORITY	3. DISTRIBUTION/AVAILABILITY OF REPORT Approved for public release; distribution unlimited
2b. DECLASSIFICATION/DOWNGRADING SCHEDULE	
4. PERFORMING ORGANIZATION REPORT NUMBER(S) AFGL-TR-87-0081 ERP, No. 970	5. MONITORING ORGANIZATION REPORT NUMBER(S)
6a. NAME OF PERFORMING ORGANIZATION Air Force Geophysics Laboratory; 6b. OFFICE SYMBOL (If applicable) LYA	7a. NAME OF MONITORING ORGANIZATION
6c. ADDRESS (City, State, and ZIP Code) Hanscom AFB Massachusetts 01731-5000	7b. ADDRESS (City, State, and ZIP Code)
8a. NAME OF FUNDING/SPONSORING ORGANIZATION; 8b. OFFICE SYMBOL (If applicable)	9. PROCUREMENT INSTRUMENT IDENTIFICATION NUMBER
8c. ADDRESS (City, State, and ZIP Code)	10. SOURCE OF FUNDING NUMBERS: PROGRAM ELEMENT NO. 62101F; PROJECT NO. 6670; TASK NO 09; WORK UNIT ACCESSION NO 13

11. TITLE (Include Security Classification)

Estimates of Satellite EHF Communication Outages Due to Attenuation by Rain

12. PERSONAL AUTHOR(S)

Paul Tattelman, Richard W. Knight,* and Kathryn G. Scharr**

13a. TYPE OF REPORT	13b. TIME COVERED	14. DATE OF REPORT (Year, Month, Day)	15. PAGE COUNT
Scientific. Interim.	FROM 1986 TO	1987 March 5	42

16. SUPPLEMENTARY NOTATION *National Climatic Data Center; Asheville, North Carolina
**Bedford Research Associates; Bedford, Massachusetts

17. COSATI CODES			18. SUBJECT TERMS (Continue on reverse if necessary and identify by block number)
FIELD	GROUP	SUB-GROUP	Rainfall rate, Attenuation, EHF communications, Satellite communications

19. ABSTRACT (Continue on reverse if necessary and identify by block number)

This report provides estimates of outage frequencies, durations, and probabilities at eight United States locations for a satellite EHF communication system employing a frequency of 30 GHz and a fade margin of 15 dB. Ten years of 1-min rain rates at each location were used in conjunction with an attenuation model to make the estimates. One-min rates are recognized as most practical for these calculations, but are ordinarily unreadable from original raingage recordings. A method for extracting the 1-min rates from original raingage recordings is described. Analyses of the 1-min rain rates and outage estimates for elevation angles of 10°, 30°, 50°, and 70° are presented.

20. DISTRIBUTION/AVAILABILITY OF ABSTRACT ☐ UNCLASSIFIED/UNLIMITED ☒ SAME AS RPT ☐ DTIC USERS	21. ABSTRACT SECURITY CLASSIFICATION Unclassified
22a. NAME OF RESPONSIBLE INDIVIDUAL Paul Tattelman	22b. TELEPHONE (Include Area Code) (617) 377-5956; 22c. OFFICE SYMBOL LYA

DD Form 1473, JUN 86 Previous editions are obsolete. SECURITY CLASSIFICATION OF THIS PAGE
Unclassified

Preface

The authors express their appreciation to Charles Glauber, USAF Environmental Technical Applications Center, for providing critical rain-rates used in our outage calculations; Jim Willand, Systems and Applied Sciences Corporation, for his data processing support; and to Mrs. Helen Connell for typing the manuscript.

Contents

Illustrations

Tables

Tables

Estimates of Satellite EHF Communication Outages Due to Attenuation by Rain

1. INTRODUCTION

Rain is a major consideration in the design of most military systems and equipment that must operate in or through the troposphere. In addition to the mechanical impact of rain (for example, erosion on the leading edges of aerospace vehicles, leakage into sealed components and so on), rain is a major cause of attenuation of microwave signals used in communications, surveillance, and weaponry. Satellite communication systems employing EHF are especially vulnerable to attenuation due to rain.

One-min rainfall rates are generally considered most practical for design considerations and as input to attenuation models. However, records of rainfall amounts for periods less than an hour are not readily available. Amounts for increments less than 5 min were primarily collected during special field programs for limited time periods, generally one to three years. This has prompted the development of numerous models to estimate frequencies of 1-min rates.[1,2]

(Received for publication 3 March 1987)

1. Tattelman, P., and Grantham, D.D. (1985) A review of models for estimating 1-min rainfall rates for microwave attenuation calculations, IEEE Trans. Commun., COM-33(No. 4):361-372.

2. Tattelman, P., and Scharr, K.G. (1983) A model for estimating 1-min rainfall rates, J. Clim. and Appl. Meteor., 22(No. 9):1575-1580.

For most mechanical design considerations involving rain, it is sufficient to know probabilities of extreme rates at locations noted for heavy rain.[3] This is because military equipment is usually designed for operation worldwide based on conditions during the worst month in the most severe part of the world for each climatic element. However, attenuation of radio signals can be significant at relatively low rain rates that occur with varying probabilities just about anywhere in the world. Therefore, statistics on the frequency and duration of 1-min rain rates are required for locations representing many climatic rainfall regimes. These can be used in attenuation models to determine required power levels, the frequency and duration of communication outages, and the need for space diversity of terminals or other alternatives. This report describes a method used for extracting 1-min rates from a largely untapped reservoir of original raingage recordings, and presents analyses of the data obtained for eight locations.

2. DATA

Weighing raingage recordings for approximately 300 first-order U.S. weather stations are archived on microfiche at the National Climatic Data Center (NCDC), Asheville, North Carolina. Our task is to build a data base of 1-min rainfall rates over a period of ten years at a number of stations. Stations are being chosen primarily to represent as many different climatic rainfall regimes as possible. Data from stations in close proximity will also be studied to determine spatial variability of 1-min rain-rate distributions and results will be presented in a future report. Note that rain rates for solid precipitation represent melted values.

Ten years of 1-min rain rate data for eight locations were analyzed for this report. The locations, the percent of time it rained at each (not including missing data), and the percent of the rain data that were missing is provided in Table 1. Missing data represent periods of rain when chart records were unavailable for digitizing. Since hourly totals were nevertheless available, it was assumed that it rained throughout the hour at the averaged rate for each minute. Therefore, the percent of missing data in Table 1 was calculated by assuming the maximum possible number of minutes of missing rain. These data were not used in any of the analyses; however, Table 1 indicates that estimated missing data for rates at or above 0.05 mm/min constitute a small fraction of the total.

---

3. Tattelman, P., and Willis, P.T. (1985) Model Vertical Profiles of Extreme Rainfall Rate, Liquid Water Content, and Drop-size Distribution, AFGL-TR-85-0200, AD A164424.

Table 1. Locations for Which 10 Years of 1-min Rain Rate Data Were Studied. The percent of time it rains (not including missing rain data), and the estimated percent of the rain data that are missing is provided

		Percent of Time it Rains					Estimated Percent of Rain Data Missing	
Location	Elevation (m)	Jan	Apr	Jul	Oct	Ann	All*	Rates ≥ 0.05 mm/min
Boston, Mass.	5	8.3	6.5	3.1	5.4	6.2	2.6	0.4
Denver, Co.	1610	1.5	4.3	1.9	2.6	2.8	3.8	0.4
Grand Junction, Co.	1475	2.7	2.0	0.8	2.1	1.8	4.0	0.1
Key West, Fla.	3	1.7	0.9	2.5	2.7	2.2	5.5	0.4
Omaha, Neb.	390	2.4	4.7	2.5	3.7	3.2	16.0	1.3
Rapid City, S.D.	955	1.9	5.4	2.5	2.6	2.9	8.7	0.6
Seattle, Wash.	120	13.8	6.4	2.3	7.3	7.9	3.0	0.0
Urbana, Ill.	175	4.7	4.1	2.7	3.6	4.1	1.23**	

*These values constitute the maximum possible (see text)

**This value represents percent of full-operational time

The data at all locations except Urbana were obtained from raingage recordings stored at NCDC for the period 1 January 1970 to 31 December 1979. The data for Urbana were obtained from the Illinois State Water Survey, Champaign, Illinois as part of a USAF contract.[4,5] The Urbana data cover a period of 10.25 years from 1 June 1969 to 31 August 1979. They were obtained using a high-speed weighing raingage recorder described in the references.

3. EXTRACTION OF 1-MIN RATES

The trace on a weighing raingage chart (Figure 1) is the representation of the integral of the rainfall rate over time. To obtain rates, we differentiate the function that describes the trace at each point of interest, that is, at each minute.

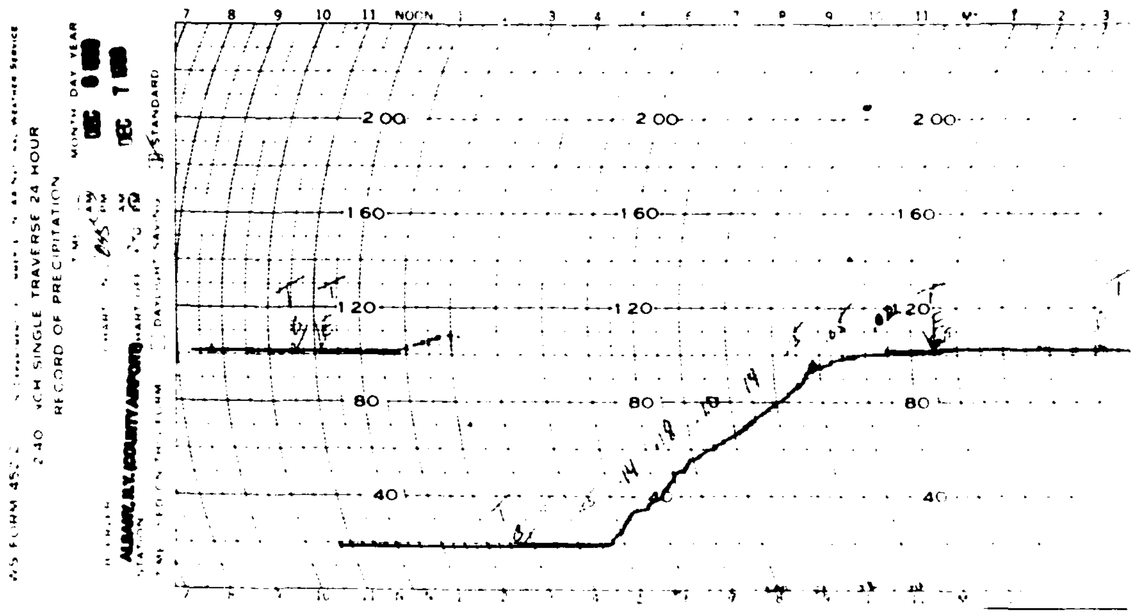

Figure 1. Standard Weighing Raingage Trace (smaller than original)

4. Jones, D.M.A., and Wendland, W.M. (1983) Statistics of Instantaneous Rainfall Rates, Final report for contract F19628-82-K-0012, AFGL-TR-83-0056, AD A130089.

5. Jones, D.M.A., and Wendland, W.M. (1984) Some statistics of instantaneous precipitaion, J. Clim. and Appl. Meteor., 23:1273-1285.

[illegible]

[illegible] The process of eliminating these errors is described in two articles by Ruthroff and Bodtmann[6] and Bodtmann and Ruthroff.[7] The processing used for this data set is essentially as recommended in those articles.

3.1 Digitization

Hourly rainfall amounts for all U.S. first-order weather stations are published monthly by NCDC in Local Climatological Data. This publication was used to determine periods of measurable rain at selected stations. Paper copies of the microfiche records for these periods were enlarged to more than twice their original size. The original chart has a resolution of 0.2 mm per min (for example, a 15-min time interval is 3-mm long). Our trial tests showed that we could consistently digitize points with a repeatability of ±0.1 mm that corresponds to ±0.5 min on original size charts. By expanding the charts to a resolution of 0.428 mm per min we have essentially halved the uncertainty in the time-axis measurements to a quarter of a minute.

Each precipitation trace is sampled using the incremental stream mode of the digitizing tablet. This means that a point is recorded each time the cursor is moved a prescribed distance along the trace, that in this application is set at 0.25 mm. Therefore, during low rainfall rate episodes (flat trace) points are sampled at approximately half-min intervals. During high-rate episodes (sharp curve) the points are sampled at smaller intervals of time, thus the sampling rate per min is much higher.

---

6. Ruthroff, C.L., and Bodtmann, W.F. (1976) Computing derivatives from equally spaced data, J. Appl. Meteor., 15:1152-1159.

7. Bodtmann, W.F., and Ruthroff, C.L. (1976) The measurement of 1-min rain rates from weighing raingage recordings, J. Appl. Meteor., 15:1160-1166.

3.2 Processing

For reasons discussed earlier, we know that the computations of rainfall rates will be contaminated by a high-frequency noise component induced by small inaccuracies in the digitized representation of the trace. Our goal is to remove the noise and recover the signal. This is done by employing a suitable low-pass filter.

The computational steps that were employed in our 1-min rain rate processing were based on the procedures in Ruthroff and Bodtmann.[6] They are:

(1) Half-min interpolation. Linear interpolation is used to produce both an x- and a y-coordinate value for each half-min increment of the precipitation episode. Digitizing errors occur with equal likelihood in x and y. However, the interpolation procedure forces all of the error onto the y coordinate only, that simplifies subsequent processing.

(2) Running mean smoother. A three-point running mean smoother is applied to the half-minute data to ameliorate the effects of some of the larger inconsistencies.

(3) Detrend trace. This allows the data representing the precipitation trace to be expanded into a finite Fourier series.

(4) Fourier expansion. The detrended data are converted from the time domain into the frequency domain by use of a Fast Fourier Transform (FFT).

(5) Fourier filter. Filtering is accomplished by disregarding all of the Fourier coefficients that fall beyond the filter cutoff and then reconstructing the precipitation trace with the coefficients that remain.

(6) Final smoother. A cubic spline smoother is invoked to eliminate residual sinusoidal components resulting from the filter.

(7) Rate computation. The filtered trace is made monotonically increasing to eliminate negative rainfall rates. One-min rates are computed and those less than 0.25 mm per hr are set to zero.

3.2.1 FILTERING AND SMOOTHING

3.2.1.1 Fourier Expansion

Any stationary time series can be transformed from the time domain to the frequency domain by the following:[8]

---

8. Bloomfield, P. (1976) Fourier Analysis of Time Series: An Introduction, John Wiley & Sons, Inc., 258 pp.

$$X_t = A_o + \sum (A_j \cos \omega_j t + B_j \sin \omega_j t) \qquad (1)$$

$$o < j \leqq n/2$$

where X_t represents values at time t, A_o is the mean of the time series, ω is the Fourier frequency, and A_j and B_j are coefficients. Each point X_t of the function is calculated by summing sines and cosines of each of the j Fourier frequencies and weighting each by a Fourier coefficient (A_j, B_j). The Fourier frequencies ω_j can be thought of as having the dimension of cycles per unit of time ($\omega_j = 2\pi\ j/n$) where n is the number of data points. Since it takes a minimum of two points to represent the shortest cycle, there can be a maximum of n/2 Fourier frequencies. In this application, we have data values equally spaced at half-minute intervals. Therefore, a precipitation episode lasting, say 2 hrs, will have 240 points. (Episodes range from 1 to 8 hrs for our filtering process.) The highest resolvable frequency will be at $j = 240/2 = 120$ and will have a value of $\omega_j = 120/240 = 0.5$ cycles per half minute or 1 cycle per minute. The lowest frequency, of course, is always 1 cycle per total period, which in this example corresponds to a wavelength of 2 hours. Thus, a Fourier decomposition of our 2-hr episode consists of waves having periods from 1 min to 2 hrs.

The fact that a digitized precipitation trace can be represented as a combination of contributions from many wavelengths makes the Fourier transform attractive as a filtering tool. We now have a means to separate the contributions supplied by the short wavelength noise from the longer wavelength contributions associated with the real precipitation episode.

3.2.1.2 Fourier Filter

The Fourier expansion of the detrended precipitation trace yields n/2 Fourier coefficients. Low-pass rectangular filtering is accomplished by setting to zero all of the A_j and B_j coefficients beyond the j that is chosen as the filter cutoff. The obvious question is, where does one place the filter cutoff?

To obtain insight into which frequencies contribute most to the signal, we compute the following function:

$$I(\omega_j) = \frac{n}{8\pi} (A_j^2 + B_j^2) \text{ for } j = 1, 2, \ldots n\ , \qquad (2)$$

where n is the number of half-minute intervals and A_j and B_j are coefficients in Eq. (1). The plot of log $[I(\omega_j)]$ versus j, known as the periodogram,[8] is used because the variation between frequencies is generally several orders of magnitude. The signal spectrum will decrease rapidly to a flatter, randomly oscillating spectrum resulting from noise.[6] The filter cutoff should be placed at the intersection where the steep meets the flatter portion of the curve. An example of a periodogram with the filter cutoff represented by a dashed line is shown in Figure 2.

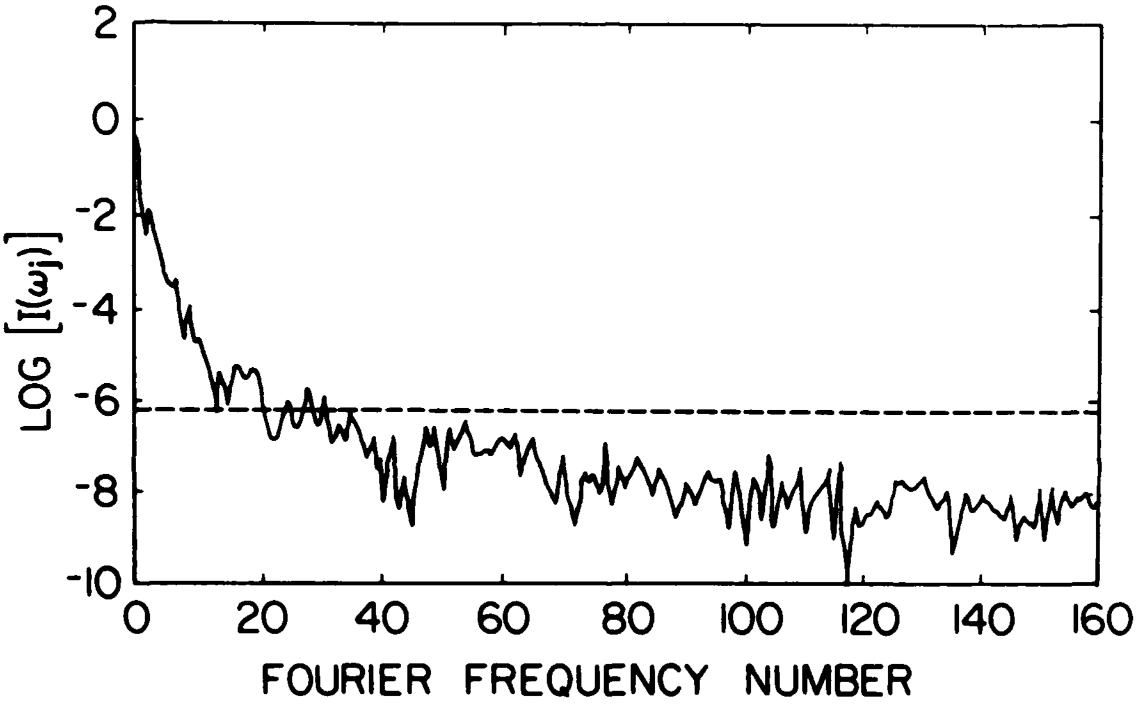

Figure 2. Example of a Periodogram Used to Determine Fourier Frequency Cutoff

3.2.1.3 Cubic Spline Smoother

When the precipitation trace is reconstructed without the shorter wavelengths associated with noise, the filtered trace may display a very subtle sinusoïdal oscillation. This, of course, is an artifact resulting from the sine-cosine basis used in the Fourier decomposition. While the total effect upon the rate computations is small, it does give a time series of computed rates a rather unnatural appearance. Therefore, a cubic spline smoothing routine with a variable sensitivity parameter is used to mitigate the oscillation.

3.2.2 TUNING FOR OBJECTIVE ANALYSIS

Section 3.2.1.2 explains the method for selection of the filter cutoff parameter. However, visual inspection of the periodogram for each of the thousands of precipitation episodes that are being processed is clearly impractical. Therefore, an automated parameter selection criterion that is optimized for high precipitation rates was instituted.

Two simulated precipitation episodes were used to determine the characteristic noise structure associated with manually digitizing high-rate precipitation. Each trace was digitized ten times by the same person. As expected, the rate computations were quite noisy and there was a rather large variability in the value for the maximum 1-min rate. Figure 3 shows the effects of various processing steps on the magnitude of the maximum 1-min rate for one of the episodes. The uncorrected mean was 1.27 mm/minute. When all of the processing steps were used (curve d in Figure 3), the values for the maximum rate stabilized around the corrected value of 1 mm/minute.

Based on these two sets of trials, cutoff parameters were chosen that were a function of the length of the precipitation episode, that, for our filtering process, ranged from 1 to 8 hours. The value of the parameter begins at -5.5 for a 1-hr event and decreases in increments of 0.1 for each additional hour in the time series. The cutoff selection criteria were validated by many experiments using actual digitized data and various analytic functions.

Normally, a single pass will be made through the filtering and smoothing routines. However, a check is made to determine the maximum 1-min difference in rate between the filtered and unfiltered data. This is done to ensure that the filter hasn't excessively smoothed a high-rate precipitation event. If the maximum difference exceeds 0.25 mm/min, an additional filter iteration is invoked. The filter cutoff parameter is decreased by 0.1 and new rates are computed. This process continues, if necessary, for a maximum of three iterations.

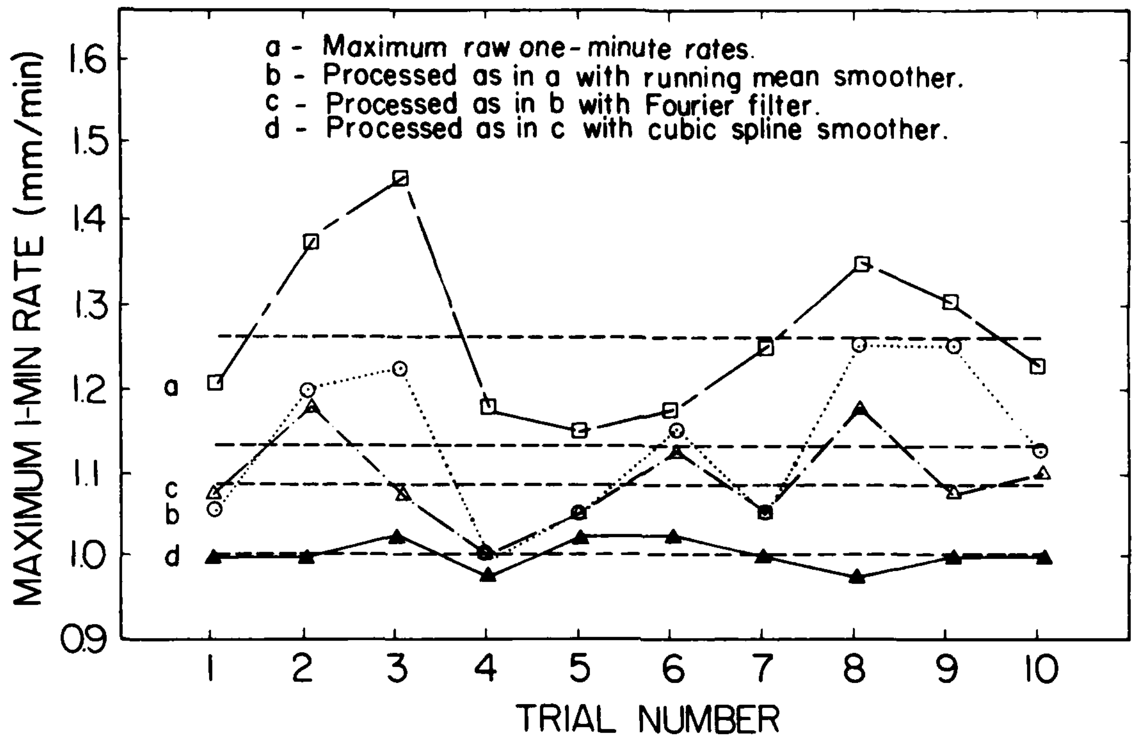

Figure 3. Effects of Various Processing Steps on the Computed Maximum 1-min Precipitation Rate

As a final check, the experiment conducted in R-B[6] was repeated. In that experiment, white noise was added to the function

$$y = 1 - \exp(-2x^3)$$

and rates were computed before and after filtering. The filter was able to recover the original signal with a high degree of accuracy. Our processing steps were also very successful in recovering the original signal.

3.3 Quality Control

In order to ensure a high-quality data set, we have employed extensive quality control procedures. The digitized data are scrutinized in four places during the processing, two before filtering and two after. The checking procedures are:

(1) Checks During Digitizing. The first checking occurs in the digitization program. The technician is asked to verify the header containing all of the housekeeping information that was entered for the trace. The program then performs a check on the length of the episode and the technician verifies the computed totals for length of time and precipitation amount.

(2) Checks During Data Transfer. During the data transfer from our data entry computer to the data processing computer, each trace is displayed on a graphics CRT. The housekeeping information is again checked, and the shape of the digitized trace is compared to the original. Traces having errors are marked for deletion at this point.

(3) Checks Against Published Data. The 1-min rates resulting from the processing program are summed by the hour, printed, and then compared to the amounts published in Local Climatological Data.

(4) Checks on Extreme Values. The final quality control step is used to check extreme or possibly anomalous data. An entry in a log file is automatically made if one or more of three criteria are met. The three criteria are: (1) high precipitation rate ($\geqq$ 1.25 mm/min); (2) a large discrepancy in the maximum precipitation rate between filtered and unfiltered data ($\geqq$ 0.5 mm/min); and (3) excessively short wavelengths used in the reconstruction of the trace after filtering ($\leqq$ 2.5 min).

4. ANALYSES OF 1-MIN RATES

The analyses of 1-min rates presented here are intended primarily to assess the impact of rain on EHF communications. Most previous studies of short-duration rain rates for use in attenuation models provide data in the form of annual rain-rate frequencies.[1] However, annual statistics can be very misleading because critical rates are concentrated in only a few months of the year at most locations. A low annual frequency of a critical rate can be intolerably high in these months. Although annual rain-rate frequencies are presented for each location studied, monthly or seasonal rain-rate statistics are preferable for assessing the impact of attenuation caused by rain.

4.1 Rain-rate Duration Frequencies

Annual average rain-rate frequencies for six duration times are provided for each location in Figures 4 and 5. Rain rates are equalled or exceeded during each minute of the specified duration. Actual frequencies are plotted for every 0.05 mm/min rate up to 1.00 mm/hr and for every 0.10 mm/min thereafter. Values plotted for a frequency of 10^{-2} represent the highest rate that was equalled or exceeded for the specified duration.

Monthly average rain-rate frequencies (for six different duration times) are provided for the worst (most extreme) month at each location in Figures 6 and 7. Values are plotted in the same manner as Figures 4 and 5. The worst month at each location was subjectively chosen from all the monthly plots to "generally" represent the highest frequencies of rates for all durations. Frequencies for some rates and durations may be higher in other months.

To get an appreciation of how the frequency of 1-min rates varies during the year, Figures 8 and 9 provide monthly average frequencies of 1-min rates for mid-season months. Frequencies of high rates are generally greatest during July at most locations when heavy convective showers are most common. Variability is least for Key West and Seattle where rates are relatively high and low, respectively, during each of the months.

4.2 Rain-rate Duration Probabilities

For many design considerations it is more practical to express the likelihood of events in terms of their probability. The Poisson distribution is an appropriate tool for quantifying random events, such as rainfall occurrences, if the events in any time interval are statistically independent of events in another time interval. In this case, rain events are 5-, 10-, 15-, 20-, and 30-min durations and the time interval is a specified month of the year (for example, July). Since these rain events are independent, the probability, P, of y rain events in a month can be calculated using the Poisson formula

$$P(y) = \frac{e^{-\lambda}\lambda^{y}}{y!} \tag{3}$$

where λ is the mean number of events per month. Therefore, the probability of <u>at least</u> y occurrences of an event is

$$P(\text{at least } y) = 1 - \sum_{z=0}^{y-1} P(z) \, .$$

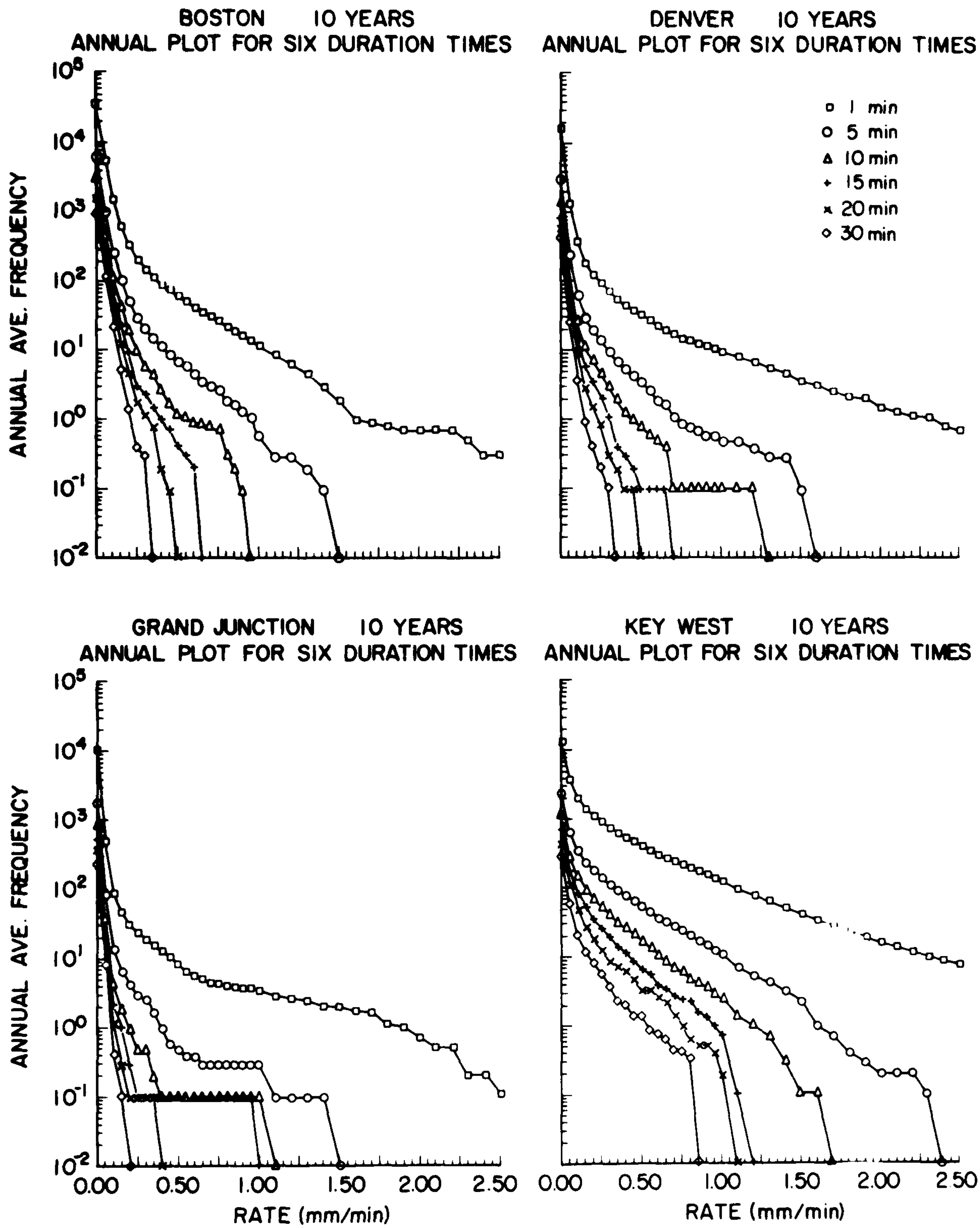

Figure 4. Average Annual Frequency of 1-min Rain Rates for Six Duration Times at Boston, Denver, Grand Junction, and Key West

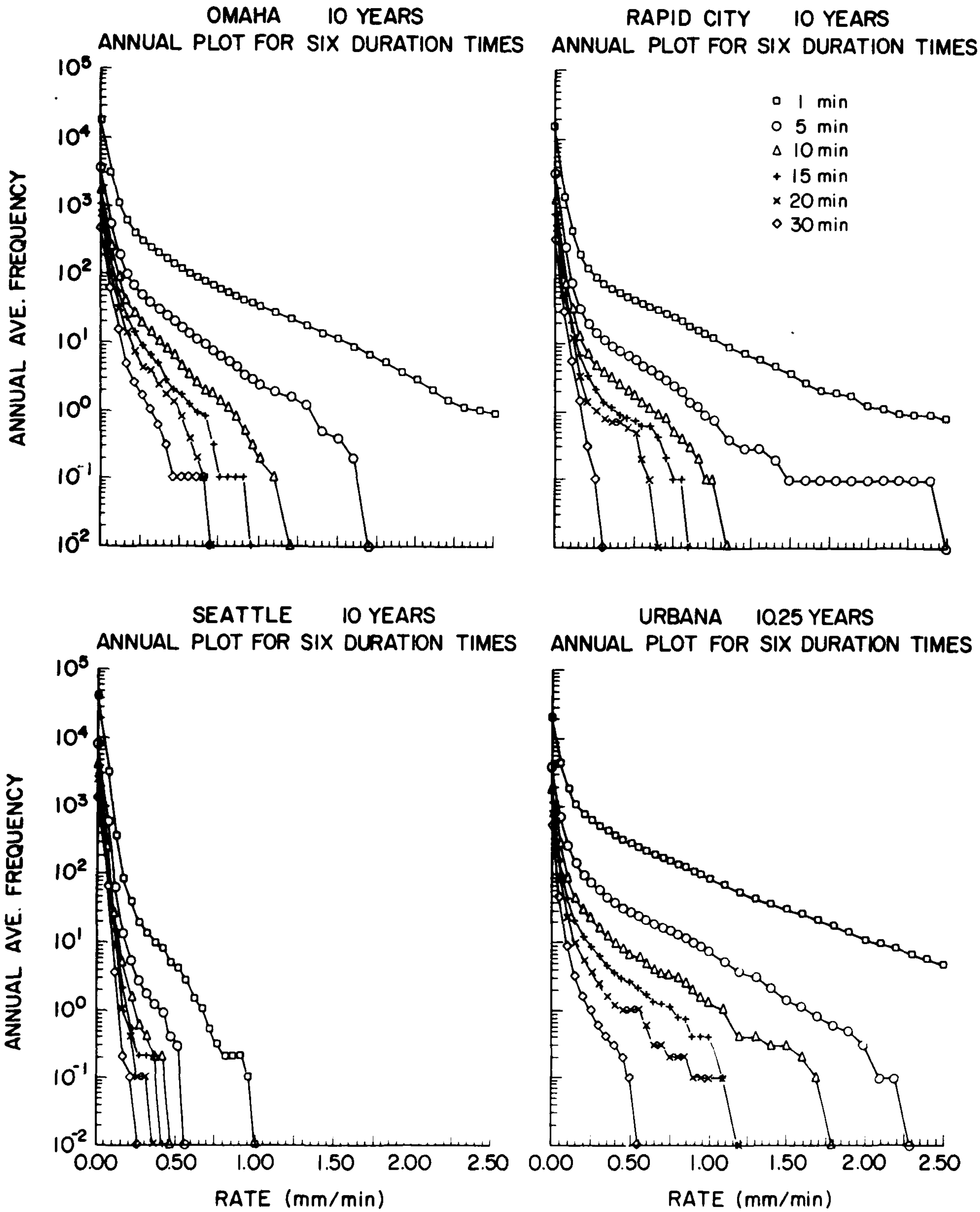

Figure 5. Average Annual Frequency of 1-min Rain Rates for Six Duration Times at Omaha, Rapid City, Seattle, and Urbana

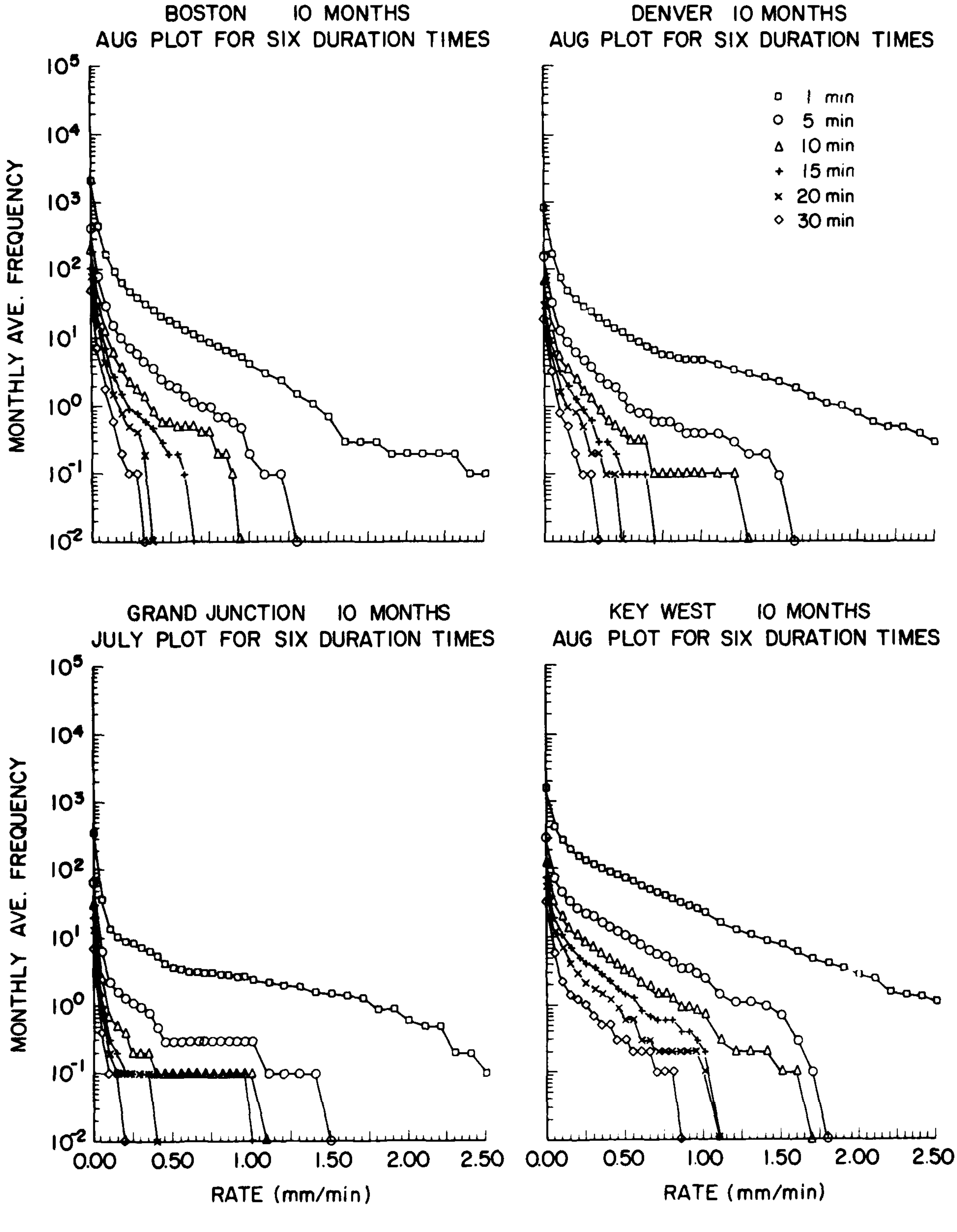

Figure 6. Average Worst-month Frequency of 1-min Rain Rates for Six Duration Times at Boston, Denver, Grand Junction, and Key West

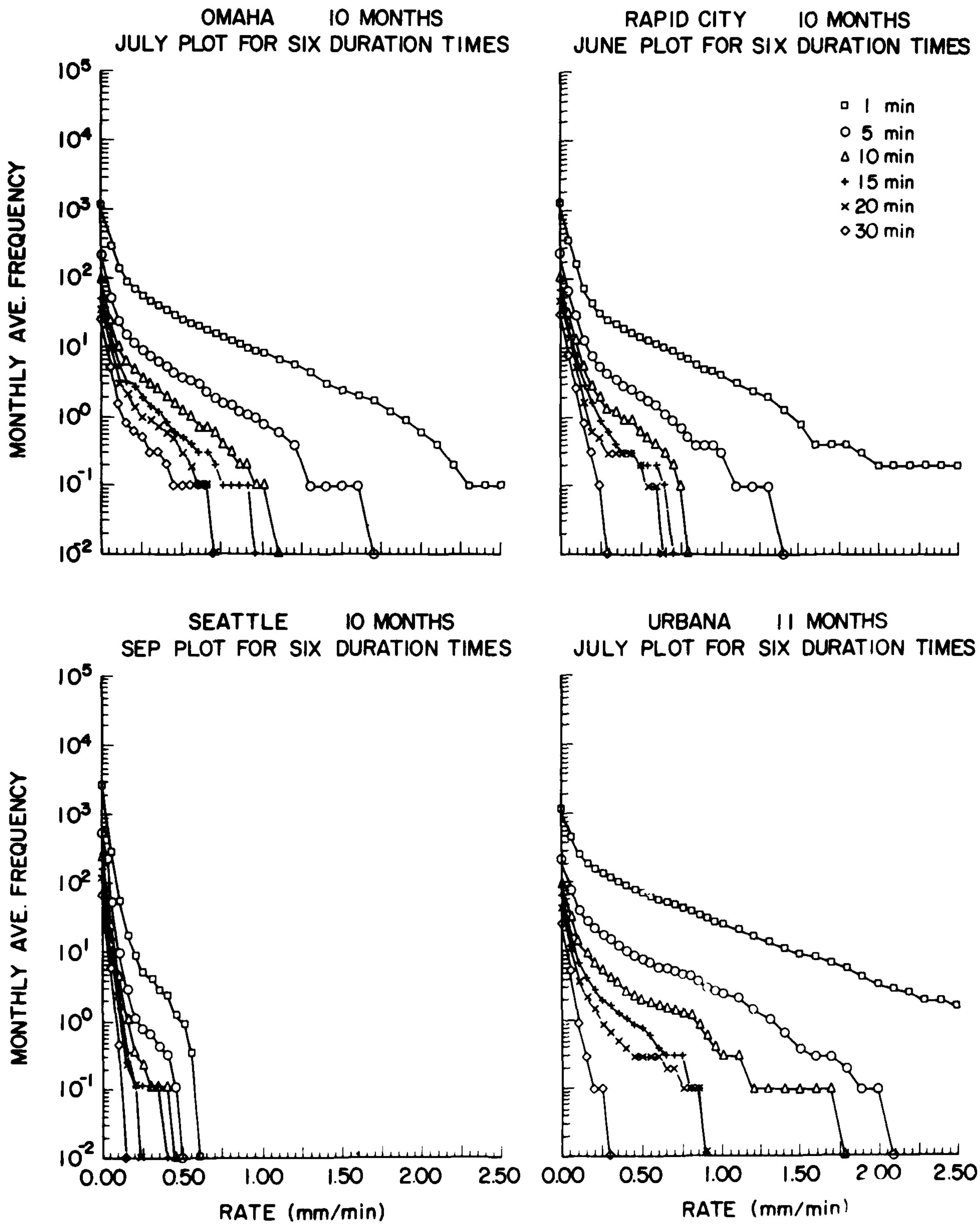

Figure 7. Average Worst-month Frequency of 1-min Rain Rates for Six Duration Times at Omaha, Rapid City, Seattle, and Urbana

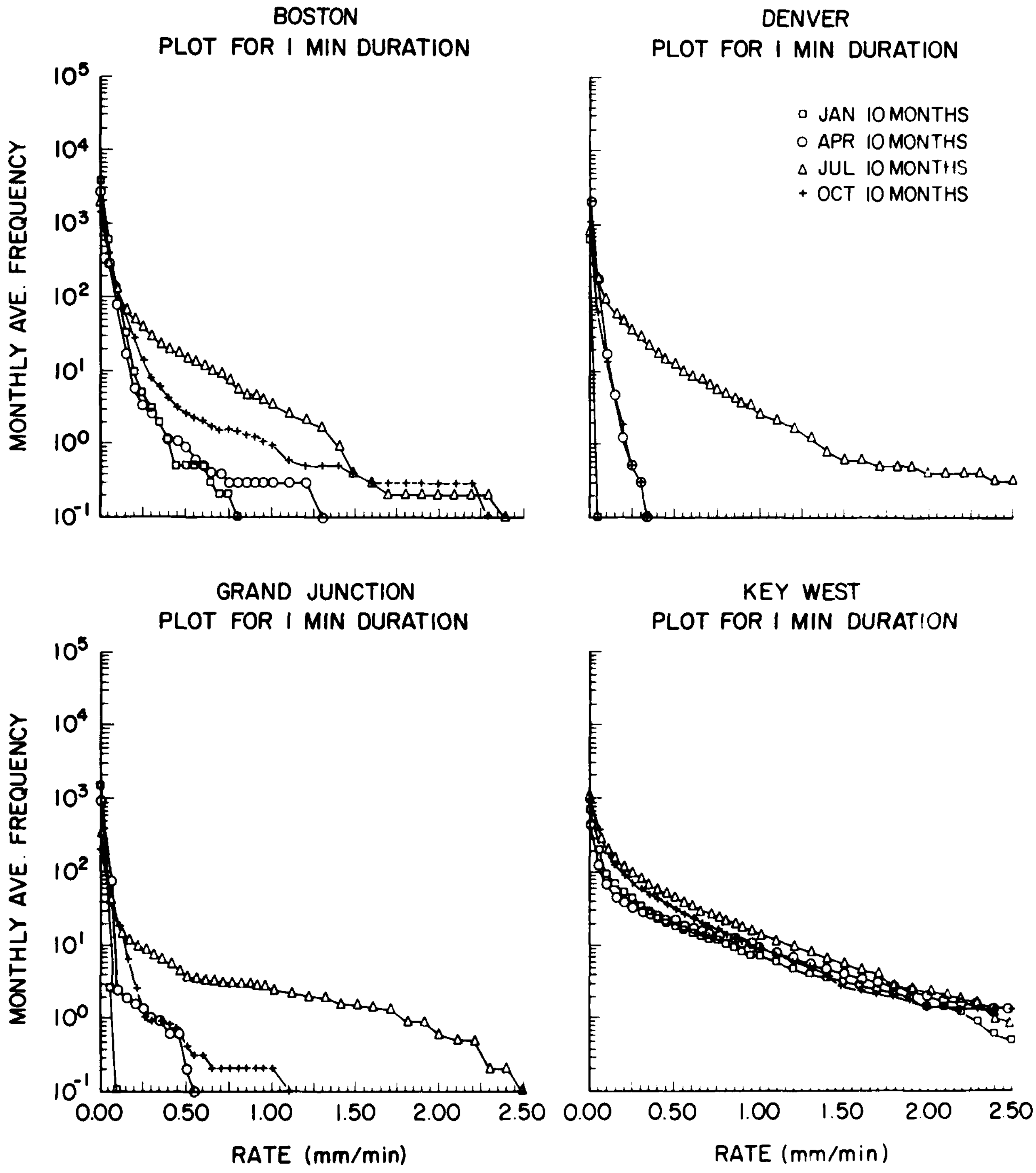

Figure 8. Average Frequency of 1-min Rain Rates for Mid-season Months at Boston, Denver, Grand Junction, and Key West

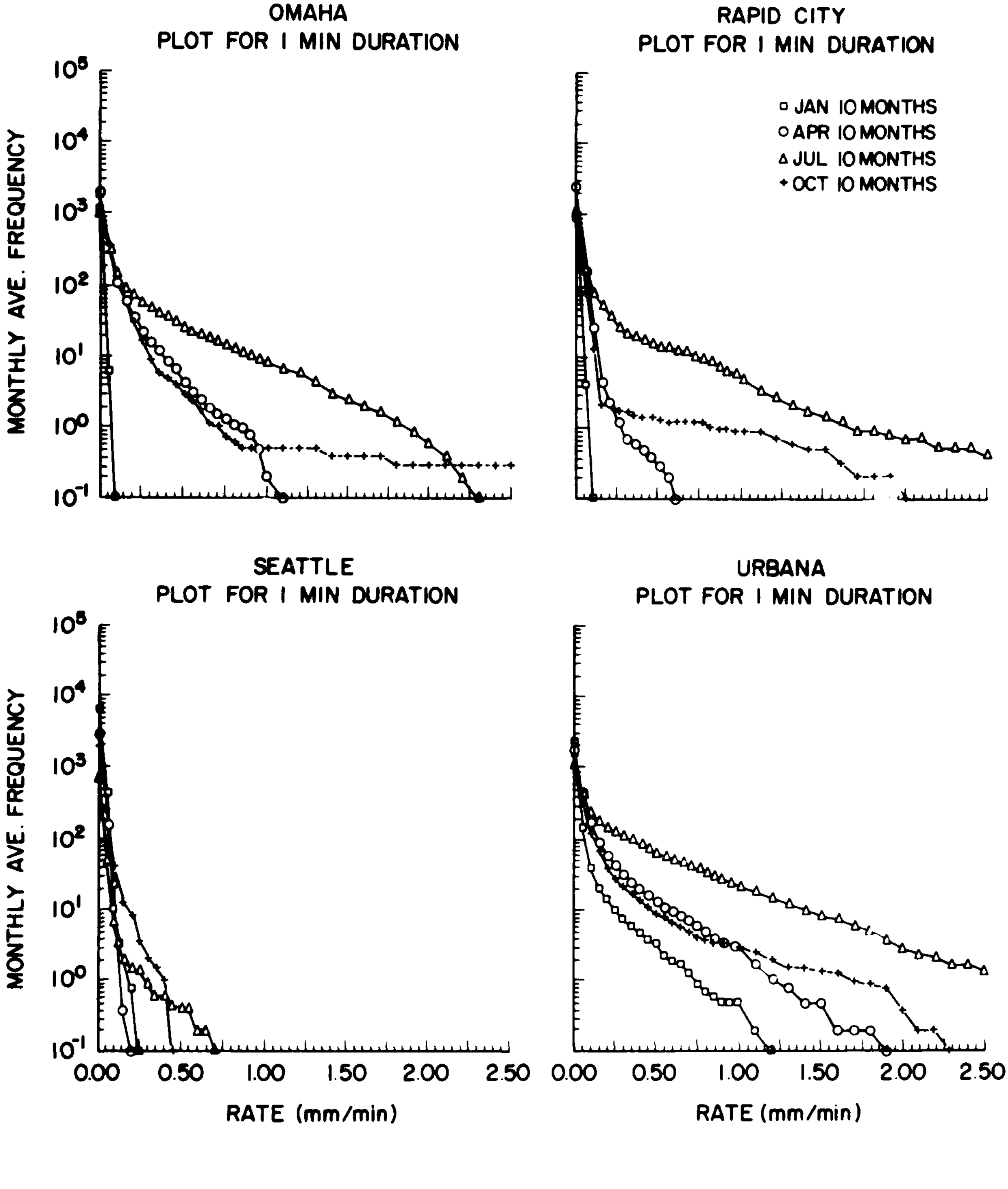

Figure 9. Average Frequency of 1-min Rain Rates for Mid-season Months at Omaha, Rapid City, Seattle, and Urbana

One-min rainfall rates versus duration and the probability of at least one occurrence during the worst month are provided in Table 2. Rates corresponding to the probability of at least three occurrences during the worst month are provided in Table 3. The worst (most severe) month was subjectively chosen to "generally" represent the highest rates for each probability and duration. Rates for some probabilities and durations may be higher in other months.

Table 4 presents the longest duration at or above specified threshold rain rates and the month of the year that it occurred. Since these are the most extreme occurrences in 10 years (10.25 years at Urbana), the probability that they would occur in that month in any one year is approximately 0.1.

4.3 Time Between Events

To more completely assess the impact of an attenuation outage due to rain, it is also important to know how soon an outage may recur. That is, if it is raining at or above a critical rate then drops below that rate, what time period would elapse before the rate was exceeded again? We call the period of time between the occurrence of specified rates the time between events (TBE). For this study, we considered five threshold rates, 0.10, 0.25, 0.50, 0.75 and 1.00 mm/min, that were equalled or exceeded for each of 5 (and 10) consecutive minutes. Each rate and duration constitutes an event, for a total of five 5-min events and five 10-min events. When an event occurs (for example, a rate of at least 0.10 mm/min for 5 consecutive min), what is the TBE until this event recurs?

The TBE's at each location were determined for each meteorological season (for example, summer is June, July, and August). The first and last TBE for each season was determined by scanning up to 30 days prior to the beginning and after the end of the season. For example, if the first event occurred on 5 June, the first TBE is determined by looking back up to 30 days to the previous event at that threshold rate and duration. If there was no prior event within the 30-day scan, the TBE is considered to be greater than 30 days and is lumped with other TBE's greater than 30 days.

Table 2. One-min Rainfall Rate Versus Duration and Probability of at Least One Occurrence During the Worst Month*

Location	Worst Month*	Rainfall Rate (mm/min) Duration (min) 5 Probability 0.1	5 0.5	5 0.9	10 Probability 0.1	10 0.5	10 0.9	15 Probability 0.1	15 0.5	15 0.9	20 Probability 0.1	20 0.5	20 0.9	30 Probability 0.1	30 0.5	30 0.9
Boston, Mass.	Aug	1.20	0.85	0.48	0.90	0.43	0.25	0.60	0.33	0.16	0.31	0.22	0.13	0.30	0.14	0.09
Denver, Co.	Aug	1.50	0.68	0.38	1.20	0.38	0.22	0.65	0.28	0.13	0.45	0.22	0.09	0.30	0.12	0.06
Grand Junction, Co.	Jul	1.40	0.37	0.10	1.00	0.10	0.06	0.95	0.07	0.05	0.35	0.06	0.04	0.20	0.05	0.03
Key West, Fla.	Aug	1.70	1.50	1.03	1.60	1.00	0.59	1.01	0.65	0.40	1.00	0.48	0.24	0.80	0.30	0.10
Omaha, Neb.	Jul	1.60	1.06	0.65	1.00	0.66	0.37	0.90	0.43	0.22	0.65	0.36	0.14	0.65	0.18	0.09
Rapid City, S.D.	Jun	1.30	0.75	0.47	0.75	0.48	0.23	0.65	0.29	0.17	0.60	0.19	0.14	0.25	0.16	0.10
Seattle, Wash.	Sep	0.45	0.30	0.17	0.40	0.17	0.13	0.35	0.13	0.10	0.20	0.12	0.09	0.12	0.09	0.07
Urbana, Ill.	Jul	2.00	1.39	1.00	1.70	0.87	0.41	0.85	0.51	0.22	0.85	0.29	0.14	0.25	0.11	0.07

*See text for definition of worst month

Table 3. One-min Rainfall Rate Versus Duration and Probability of at Least Three Occurrences During the Worst Month*

Location	Worst Month*	5			10			15			20			30		
		Probability 0.1	0.5	0.9	Probability 0.1	0.5	0.9	Probability 0.1	0.5	0.9	Probability 0.1	0.5	0.9	Probability 0.1	0.5	0.9
Boston, Ma.	Aug	0.67	0.44	0.32	0.37	0.23	0.17	0.23	0.15	0.12	0.18	0.12	0.09	0.12	0.09	0.06
Denver, Co.	Aug	0.52	0.35	0.23	0.33	0.20	0.10	0.22	0.11	0.07	0.14	0.08	0.05	0.09	0.06	0.03
Grand Junction, Co.	Jul	0.25	0.09	0.06	0.08	0.05	0.03	0.06	0.04	0.02	0.05	0.03	0.02	0.04	0.02	0.01
Key West, Fla.	Aug	1.30	1.00	0.75	0.82	0.56	0.37	0.57	0.36	0.19	0.41	0.22	0.12	0.23	0.09	0.06
Omaha, Neb.	Jul	0.90	0.62	0.41	0.52	0.33	0.18	0.36	0.20	0.10	0.24	0.12	0.08	0.12	0.08	0.05
Rapid City, S.D.	Jun	0.65	0.43	0.25	0.36	0.21	0.15	0.23	0.16	0.12	0.17	0.12	0.09	0.13	0.09	0.07
Seattle, Wash.	Sep	0.20	0.15	0.11	0.15	0.12	0.07	0.12	0.09	0.06	0.11	0.08	0.05	0.08	0.06	0.03
Urbana, Ill.	Jul	1.26	0.91	0.63	0.80	0.38	0.23	0.37	0.20	0.12	0.22	0.12	0.08	0.09	0.07	0.05

Rainfall Rate (mm/min); Duration (min)

*See text for definition of worst month

Table 4. Longest Duration of 1-min Rates at or Above Specified Threshold Rates and the Month of Occurence

	Duration (min) and Month								
	Threshold Rate (mm/min)								
Location	0.1	0.2	0.4	0.7	1.0	1.3	1.6	2.0	2.5
Boston, Ma.	275 Jan	52 Sep	23 Sep	13 Sep[1]	7 Jul[2]	7 Jul	3 Oct	3 Oct	1 Oct[2]
Denver, Co.	162 Jun	47 Aug	20 Aug	13 Aug	12 Aug	6 Aug	4 Aug[1]	4 Jul	3 Jul
Grand Junction, Co.	40 Jul	24 Jul	19 Jul	17 Jul	10 Jul	8 Jul	4 Jul	2 Jul	1 Jul
Key West, Fla.	156 May	74 Aug	61 Apr	39 Apr[1]	22 Aug	12 Aug[1]	10 Aug	7 Jul[1]	4 Jul[1]
Omaha, Neb.	142 May	67 Jul	42 Jul	18 Jul	12 Jul[1]	9 Jul	5 Jul[1]	3 Jul[3]	3 Aug[1]
Rapid City, S.D.	149 Jun	55 Jun	28 Jul	16 Jul	11 Jul	8 Jul	8 Jul	6 Jul	4 Jul
Seattle, Wash.	82 Feb	59 Oct	13 Sep	2 Aug[1]	0 -	0 -	0 -	0 -	0 -
Urbana, Ill.	91 Oct	45 May	37 May	25 Jun	20 Jun	14 Jun	10 Jul[1]	5 Jul[1]	4 May

[1] Also occurred in 1 other month

[2] Also occurred in 2 other months

[3] Also occurred in 3 other months

Continuing with this example, if there were no other events for the remainder, of the summer season, the scan stops on 31 August and a second TBE greater than 30 days is recorded. If, however, a recurrence happened on 30 August, another TBE greater than 30 days is recorded and the scan continues until the next event, or until 29 September, to determine the last TBE. If there are no more events, there are three TBE's all of which are greater than 30 days. If there are no events during an entire season, a TBE is not tallied. For TBE's up to 30 days, the exact time period is recorded.

The cumulative probability distributions of TBE for Boston, Key West, and Urbana during the season with the greatest number of events (summer) are provided in Figures 10, 11, and 12. These locations generally had the highest number of events of the sites studied. Data are not provided if a location did not have at least eight occurrences of an event. The number of events indicated in the figures are for 10 summer seasons at Boston and Key West, and 11 summer seasons at Urbana.

5. EFFECTS OF RAIN ATTENUATION ON SATELLITE COMMUNICATIONS

Ordinarily, attenuation models are used to determine path attenuation given the point rain rate. For this exercise, we reversed the order of calculation by determining critical rain-rates that would cause an outage for a specified total path attenuation of 15 dB at 30 GHz. The USAF Environmental Technical Applications Center (ETAC), Systems Support Section, provided critical rain rates based on the model developed by Crane.[9]

The propagation path length through the rain was determined using mean monthly freezing levels above the ground for the locations and months in Table 5. This table specifies the critical rates for the indicated path elevation angles at each location. Critical rates were calculated for the worst month of the year; that is, the month that generally had the highest frequency of high rain rates during the period studied. Rain intensities are highest during the summer months when freezing levels are also at their highest. Thus the number of outages is greatest during these months. The highest critical rates are at locations with the lowest freezing levels above the ground. High elevation and high latitude locations have relatively low freezing levels above the ground.

---

9. Crane, R.K. (1980) Prediction of attenuation by rain, IEEE Trans. Comm., COM-28(No. 9):1717-1733.

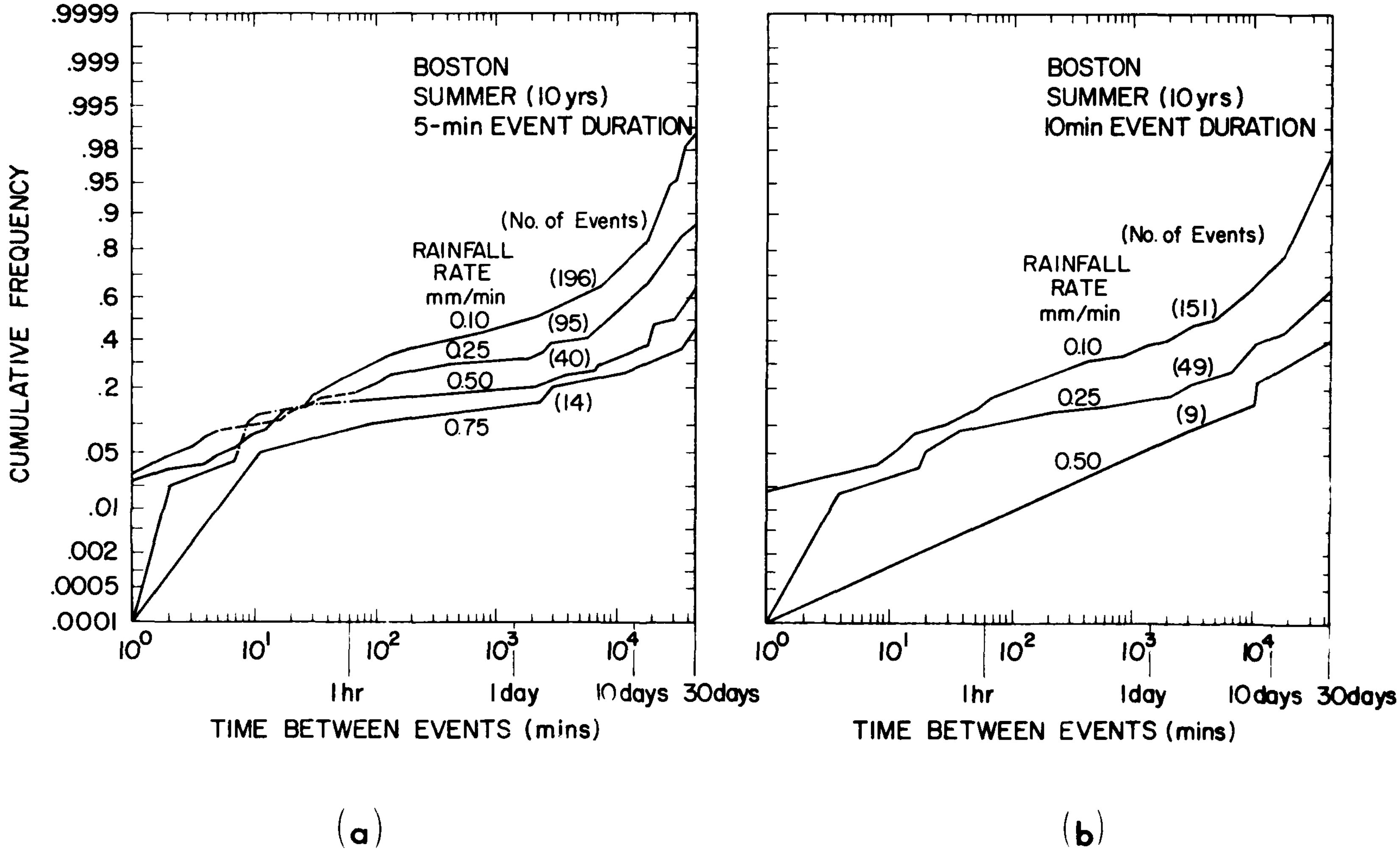

Figure 10. Cumulative Frequency Distribution of the Time Between Events Categorized by Rain Intensity at Boston During the Summer for (a) 5-min Event Duration and (b) 10-min Event Duration

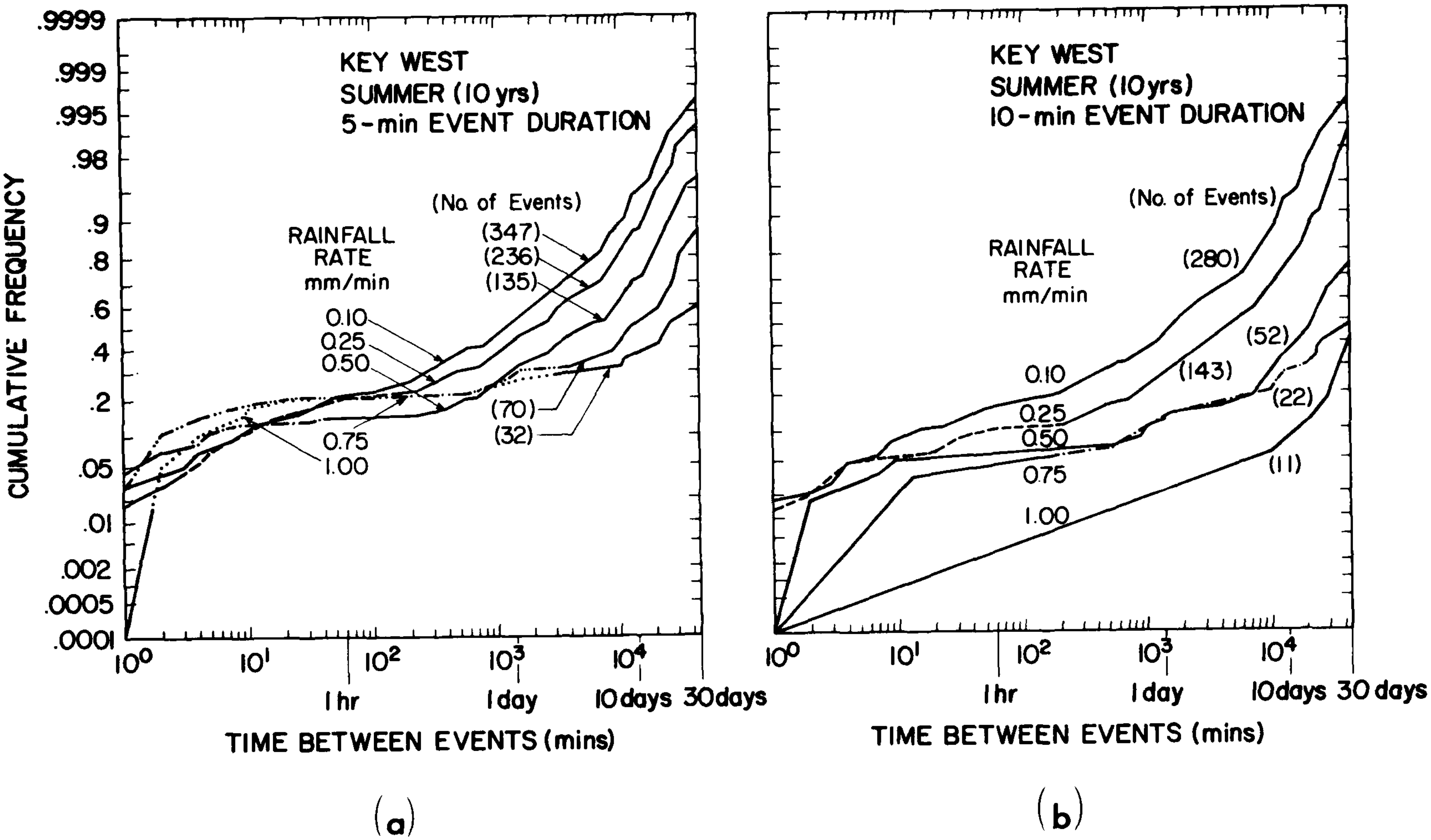

Figure 11. Cumulative Frequency Distribution of the Time Between Events Categorized by Rain Intensity at Key West During the Summer for (a) 5-min Event Duration and (b) 10-min Event Duration

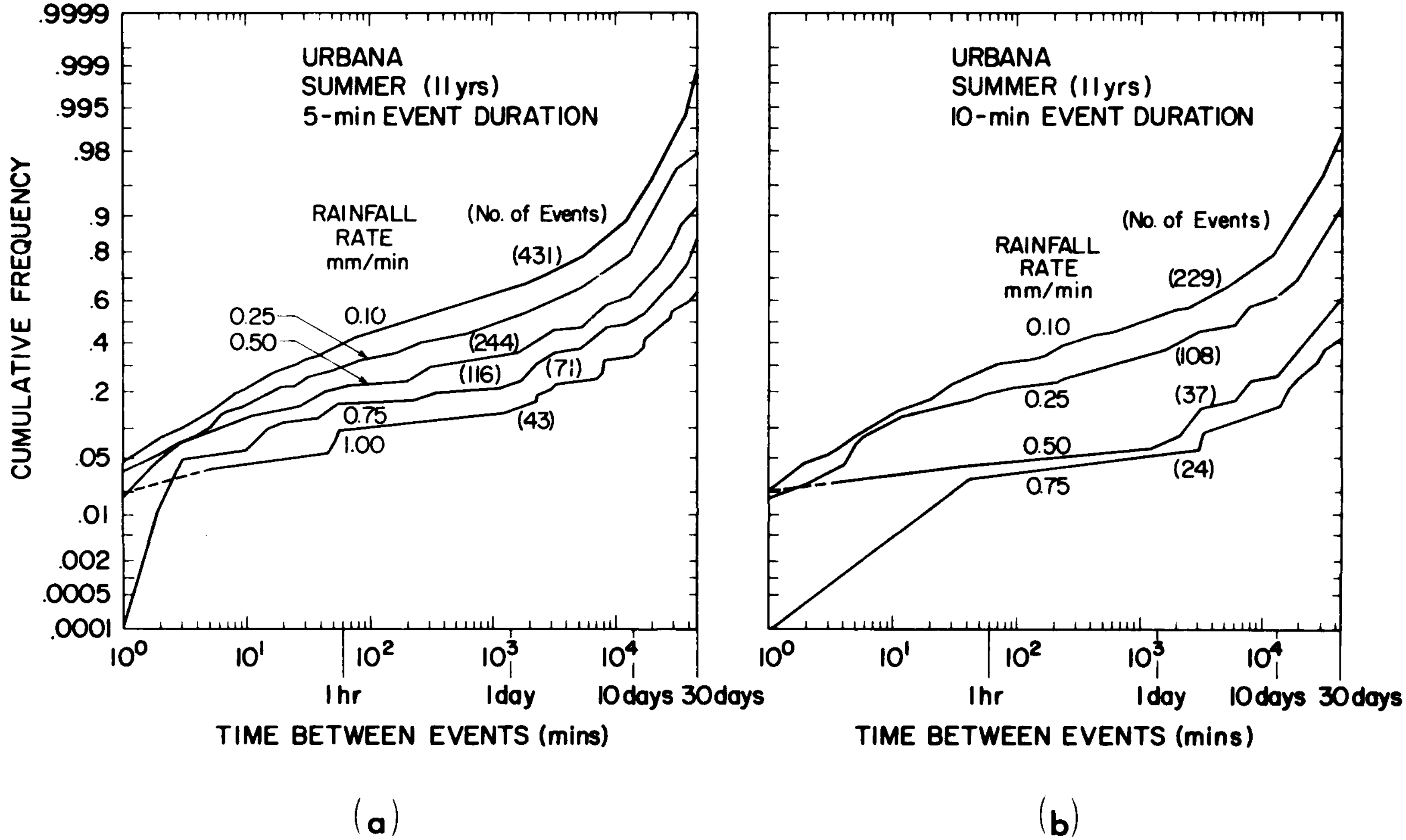

Figure 12. Cumulative Frequency Distribution of the Time Between Events Categorized by Rain Intensity at Urbana During the Summer for (a) 5-min Event Duration and (b) 10-min Event Duration

Table 6 provides the mean percent of time in the worst month with system outages due to rain. Values were estimated using the rain-rate data for 10 years at each location (11 years at Urbana), and the critical rates in Table 5. From the table it is apparent that outages due to rain are relatively infrequent. On average, one could expect system reliabilities of at least 97.5 percent at all elevation angles (not considering factors other than rain). At elevation angles of 30° and higher, the reliability increases to at least 99.3 percent.

To put the true impact of rain attenuation into perspective, it should be noted that each minute of rain is not randomly distributed in the month. When it is raining hard enough to cause an outage, it is likely to persist for a period of time. It is the duration of precipitation events causing outages that deserves special attention for EHF satellite communications.

Table 7 provides the mean number of system outages due to rain with durations of at least 5, 10, 20, and 30 min in the worst month.

At the low elevation angle of 10°, the mean number of outages lasting at least 30 min ranges from 8 to 16 at all locations except Denver and Grand Junction. The number of outages for each duration decreases rapidly with increasing elevation angle.

Table 8 provides probabilities of at least three outages due to rain in the worst month for durations of 10, 20, and 30 minutes. Here again, the elevation angle has a profound influence on the likelihood of an outage. This is especially true for Seattle which has very high probabilities of outages at 10° elevation, but very low probabilities at higher elevations.

Another important consideration is the interval between outages. The information contained in Figures 10, 11, and 12 can be used to get some valuable insight on time between outage events lasting 5 or 10 minutes. For example, in Figure 10a for 5-min rain events in Boston (summer season), cumulative frequency of time between events (TBE) is plotted for 0.10 and 0.25 mm/min. These can be used to estimate the TBE for the critical rain rates of 0.12, 0.20, and 0.27 mm/min for elevation angles of 30°, 50°, and 70°, respectively from Table 5. About 10 percent of the events during the season will recur within 10 min of another event. Between 20 and 25 percent of the events recur within an hour of another event.

At Key West (Figure 11a), about 20 percent of the 5-min events at critical rates for elevation angles of 30°, 50°, and 70° recur within an hour of another event. At Urbana (Figure 12a) 30 to 40 percent of the 5-min events at critical rates recur within an hour of another event.

Table 5. Critical Rainfall Rates Causing an Outage During the Worst Month for Stated Elevation Angles (based on a frequency of 30 GHz and a fade margin of 15 dB)

Location	Month	Mean Freezing Level (km)	Critical Rainfall Rates (mm/min) Elevation Angle 10°	30°	50°	70°
Boston, Mass.	Aug	4. 18	0. 02	0. 12	0. 20	0. 27
Denver, Co.	Aug	3. 13	0. 04	0. 17	0. 27	0. 38
Grand Junction, Co.	Jul	3. 45	0. 04	0. 15	0. 25	0. 34
Key West, Fla.	Aug	4. 69	0. 02	0. 10	0. 17	0. 24
Omaha, Neb.	Jul	4. 31	0. 02	0. 12	0. 19	0. 26
Rapid City, Neb.	Jun	2. 89	0. 05	0. 18	0. 30	0. 42
Seattle, Wash.	Sep	3. 31	0. 04	0. 16	0. 26	0. 36
Urbana, Ill.	Jul	4. 46	0. 02	0. 11	0. 18	0. 25

Table 6. Estimated Mean Percent of the Time With System Outages Due to Rain in the Worst Month for Stated Elevation Angles (based on a frequency of 30 GHz and a fade margin of 15 dB

Location	Percent of Time in the Month Elevation Angle 10°	30°	50°	70°
Boston, Mass.	2. 46	0. 32	0. 15	0. 10
Denver, Co.	0. 56	0. 11	0. 06	0. 03
Grand Junction, Co.	0. 15	0. 02	0. 02	0. 01
Key West, Fla.	2. 02	0. 63	0. 38	0. 29
Omaha, Neb.	1. 46	0. 25	0. 18	0. 13
Rapid City, S. D.	0. 81	0. 12	0. 06	0. 04
Seattle, Wash.	1. 16	0. 03	0. 01	0. 01
Urbana, Ill.	1. 68	0. 47	0. 34	0. 27

Table 7. Estimated Mean Number of System Outages Due to Rain in the Worst Month for the Indicated Durations (based on a *frequency* of 30 GHz and a fade margin of 15 dB)

	Number of Outages															
	5-min Duration				10-min Duration				20-min Duration				30-min Duration			
	Elevation Angle				Elevation Angle				Elevation Angle				Elevation Angle			
Location	10°	30°	50°	70°	10°	30°	50°	70°	10°	30°	50°	70°	10°	30°	50°	70°
Boston, Ma.	160	22	10	6.9	70	9.0	3.8	2.0	30	2.8	0.8	0.5	15	1.1	0.2	0.1
Denver, Co.	40	8.0	4.5	2.1	20	3.0	1.7	0.7	8.9	0.9	0.4	0.1	4.5	0.4	0.1	0
Grand Junction, Co.	9	1.6	1.1	0.9	3.5	0.5	0.2	0.2	1.1	0.1	0.1	0.1	0.6	0.1	0	0
Key West, Fla.	140	48	30	25	65	20	12	9.1	25	6.5	3.8	2.3	16	2.1	1.5	1.1
Omaha, Neb.	110	21	12	9.0	51	8.5	5.1	3.4	23	2.7	1.5	1.0	13	1.1	0.7	0.5
Rapid City, S.D.	70	9.0	4.1	2.8	31	3.4	1.4	0.9	14	0.8	0.3	0.3	8.0	0.4	0.1	0
Seattle, Wash.	80	2.5	0.7	0.4	31	0.9	0.2	0.1	12	0.2	0	0	8.0	0	0	0
Urbana, Ill.	130	33	23	16	55	12	7.1	5.0	20	0.2	1.5	0.8	11	0.7	0.1	0.1

Table 8. Estimated Probability of at Least Three System Outages Due to Rain in the Worst Month for the Indicated Durations (based on a frequency of 30 GHz and a fade margin of 15 dB)

	Probability of at Least Three Outages											
	10-min Duration				20-min Duration				30-min Duration			
	Elevation Angle				Elevation Angle				Elevation Angle			
Location	10°	30°	50°	70°	10°	30°	50°	70°	10°	30°	50°	70°
Boston, Ma.	0.99	0.99	0.70	0.35	0.99	0.55	0.05	0.01	0.99	0.13	0.001	*
Denver, Co.	0.99	0.61	0.20	0.04	0.95	0.07	0.006	*	0.78	0.01	*	*
Grand Junction, Co.	0.68	0.02	0.001	0.001	0.18	*	*	*	0.02	*	*	*
Key West, Fla.	0.99	0.99	0.99	0.99	0.99	0.96	0.71	0.38	0.99	0.39	0.16	0.09
Omaha, Neb.	0.99	0.99	0.88	0.68	0.99	0.50	0.20	0.08	0.99	0.13	0.03	0.01
Rapid City, S.D.	0.99	0.64	0.15	0.06	0.99	0.04	0.004	0.004	0.98	0.01	*	*
Seattle, Wash.	0.99	0.08	0.001	*	0.99	0.001	*	*	0.96	*	*	*
Urbana, Ill.	0.99	0.99	0.96	0.87	0.99	0.61	0.20	0.05	0.99	0.04	*	*

*< 0.001

6. CONCLUSIONS

Analyses of 10 years of 1-min rain data are presented for eight locations (10.25 years at Urbana). These analyses can be used to determine outage frequencies, durations, and probabilities based on critical rain rates causing an outage. The critical rates can be determined using an attenuation model such as the one developed by Crane.[9]

Based on the Crane model, critical rain rates were determined for various elevation angles for a frequency of 30 GHz and a fade margin of 15 dB at the eight locations studied. Outage statistics were estimated for each location using these and the 1-min rain rate analyses. The results show the profound influence of the elevation angle of the propagation path on the quantity and duration of outages. Lower elevation angles greatly increase the path length through the rain with outages resulting at rates as low as 0.02 mm/min at some locations.

Total path attenuation is also greatly influenced by the height of the freezing level, above which the attenuation from ice and snow is negligible. Freezing levels are lowest in the winter so that a much higher rain rate would be required to produce an outage. Of course rain rates are generally much lower during the winter months, further minimizing the likelihood of an outage. Because rain rates and freezing levels are highest during the warmest months, design of satellite EHF communications should be based on conditions during the month of the year when the frequency and duration of outages is greatest. Annual statistics that include the very low outage-probability winter months conceal the real impact of rain attenuation on operations.

References

1. Tattelman, P., and Grantham, D. D. (1985) A review of models for estimating 1-min rainfall rates for microwave attenuation calculations, IEEE Trans. Commun., COM-33(No. 4):361-372.

2. Tattelman, P., and Scharr, K.G. (1983) A model for estimating 1-min rainfall rates, J. Clim. and Appl. Meteor., 22(No. 9):1575-1580.

3. Tattelman, P., and Willis, P.T. (1985) Model Vertical Profiles of Extreme Rainfall Rate, Liquid Water Content, and Drop-size Distribution, AFGL-TR-85-0200, AD A164424.

4. Jones, D.M.A., and Wendland, W.M. (1983) Statistics of Instantaneous Rainfall Rates, Final report for contract F19628-82-K-0012, AFGL-TR-83-0056, AD A130089.

5. Jones, D.M.A., and Wendland, W.M. (1984) Some statistics of instantaneous precipitation, J. Clim. and Appl. Meteor., 23:1273-1285.

6. Ruthroff, C.L., and Bodtmann, W.F. (1976) Computing derivatives from equally spaced data, J. Appl. Meteor., 15:1152-1159.

7. Bodtmann, W.F., and Ruthroff, C.L. (1976) The measurement of 1-min rain rates from weighing raingage recordings, J. Appl. Meteor., 15:1160-1166.

8. Bloomfield, P. (1976) Fourier Analysis of Time Series: An Introduction, John Wiley & Sons, Inc., 258 pp.

9. Crane, R.K. (1980) Prediction of attenuation by rain, IEEE Trans. Comm., COM-28(No. 9):1717-1733.

END
10-81
DTIC